

Spectroscopic Studies of $z \sim 5.7$ and $z \sim 6.5$ Galaxies: Implications for Reionization

Esther M. Hu, Lennox L. Cowie, Peter Capak[†], and Yuko Kakazu

Institute for Astronomy, University of Hawaii, 2680 Woodlawn Drive, Honolulu, HI 96822, USA

Abstract. The recent development of large, complete samples which identify high-redshift galaxies at $z \sim 5.7$ and $z \sim 6.5$ from deep, wide-field surveys provides detailed information on the earliest galaxies, their numbers, spatial and kinematic distributions, and implications for early reionization of the IGM. In this contribution we present results of spectroscopic studies of $z \sim 5.7$ and $z \sim 6.5$ galaxies identified from our deep, Lyman alpha narrowband and multicolor surveys conducted with the SuprimeCam mosaic CCD camera on the 8.3-m Subaru telescope and observed with the DEIMOS multi-object spectrograph on Keck. The luminosity function of the $z \sim 6.5$ galaxies is shown to be similar to the luminosity function of the $z \sim 5.7$ galaxy samples, suggesting that a substantial star-forming population is already in place at $z \sim 6.5$. Comparisons of both individual and stacked spectra of galaxies in these two samples show that the Lyman alpha emission profiles, equivalent widths, and continuum break strengths do not substantially change over this redshift interval. The wide-field nature of the surveys also permits mapping the large-scale distribution of the high-redshift galaxies in spatial structures extending across individual SuprimeCam fields (~ 60 Mpc). Field-to-field variations in the number of objects at $z \sim 6.5$ may shortly be able to place constraints on the porosity of the reionization boundary.

Keywords. cosmology: observations — early universe — galaxies: distances and redshifts — galaxies: evolution — galaxies: formation — galaxies: high-redshift

1. Introduction

Substantial progress has been made over the last 5 years in high-redshift galaxy studies (see Spinrad (2004) for a review). The significant aspects of recent work carried out since that review are the rapid growth in the numbers of galaxies that populate the high-redshift end of the samples ($z \sim 6$ and above) and the development of large, spectroscopically complete samples from wide-area surveys for a number of discrete fields (e.g., Hu *et al.* (2004), Taniguchi *et al.* (2005), Hu *et al.* (2005)). These give a handle on the problem of cosmic variance, and also allow us to build up the large samples required for luminosity function studies. Spectroscopic completeness makes it possible to estimate the star-forming population at high redshift, and its evolution. Detailed examination and comparison of the strength and profile shape of the Ly α emission line may provide insights to possible changes in the underlying stellar population, or in the neutral hydrogen content of the surrounding intragalactic medium.

2. The Hawaii Wide-Field Narrowband Surveys

The most successful method of identifying galaxies at redshifts beyond $z \sim 5.5$, where galaxy continua are faint against a strong night sky background, is by using the redshifted Ly α emission line. The present surveys were driven by the development

[†] Present address: Department of Astronomy, California Institute of Technology, MS 105-24, 1201 E. California Blvd., Pasadena, CA, 91125, USA.

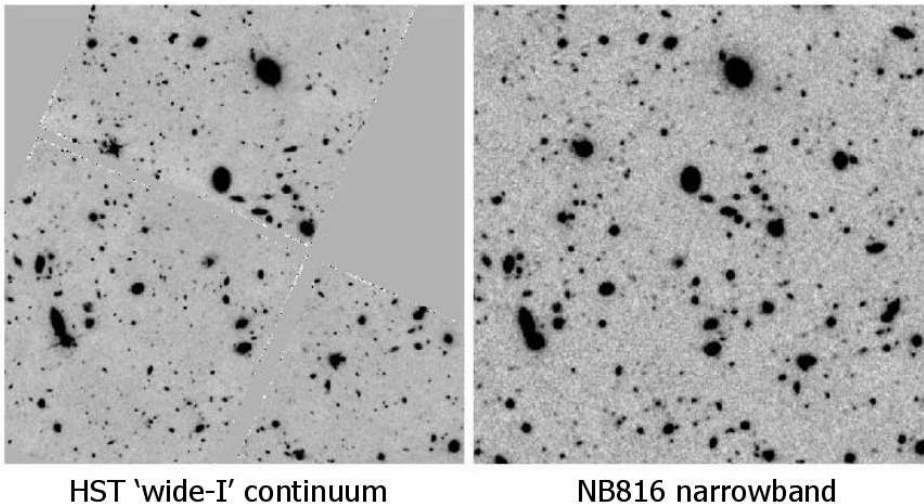


Figure 1. (*Left panel*) shows the Hubble Deep Field (HDF-N) imaged with the WFPC2 camera on HST through the F814W continuum filter. (*Right panel*) shows the same region imaged from the ground through a 120 Å-wide narrowband NB816 filter (for Ly α emission at $z \sim 5.7$) using the SuprimeCam mosaic CCD camera on Subaru. The narrowband images in the survey are comparable in depth to the HDF, and each field center surveys a region 70 times larger than the area shown here, with good image quality. Wide area coverage and image depth are required to identify and study the high-redshift samples.

of wide-field, red-sensitive instruments on the large telescopes: the half-degree FOV SuprimeCam mosaic CCD imager (Miyazaki et al. 2002) on the 8.3-m Subaru Telescope, and the wide-field ($16.7' \times 5'$) DEIMOS multi-slit spectrograph and imager on the Keck II 10-m telescope. Narrowband imaging is used in combination with deep multi-color $BVRIz'$ and moderate infrared K' imaging over the SuprimeCam fields to identify high-redshift galaxies with strong Ly α emission and continuum color breaks.

Current investigations use $\sim 120\text{\AA}$ bandpass filters centered at 8150\AA and 9130\AA (Ly α at $z \sim 5.7$ and $z \sim 6.5$) for the narrowband studies, with follow-up DEIMOS spectra (3.6\AA resolution, $R \sim 2700$) at Keck. Survey fields are chosen from half a dozen extensively studied fields: SSA22, GOODS-N, Lockman Hole NW, SSA13, SSA17, and A370. Completed studies at $z \sim 5.7$ for SSA22 (Hu *et al.* (2004)) show a high success rate in identifying and confirming candidates (19 confirmed of 22 observed), as well as success in discriminating against red stars and identifying/confirming T dwarf candidates (Kakazu *et al.* in preparation). A second $z \sim 5.7$ study has been completed for the region including the HDF-N and GOODS-N fields (Hu *et al.* (2005)). At present 62 confirmed redshifts at $z \sim 5.7$ are in hand for 3 fields, with 14 confirmed $z \sim 6.5$ redshifts (extending to $z = 6.74$) for 3 fields.

At magnitudes brighter than $AB \sim 25.5$ the number density of such high-redshift galaxies is only a few hundred per square degree and the distribution is highly correlated on sub-degree scales (e.g., Capak 2004). A combination of depth and area coverage is needed for these studies. Figure 1 shows the depth and image quality of the survey's SuprimeCam narrowband exposures compared to deep HDF continuum images. No $z \sim 5.7$ galaxies are found in the survey within the HDF-N. Over the larger ACS GOODS-N field (still a sub-region of the SuprimeCam field) only 6 $z \sim 5.7$ galaxies were found. And none of the $z \sim 6.5$ sources were found within the region of ACS GOODS-N.

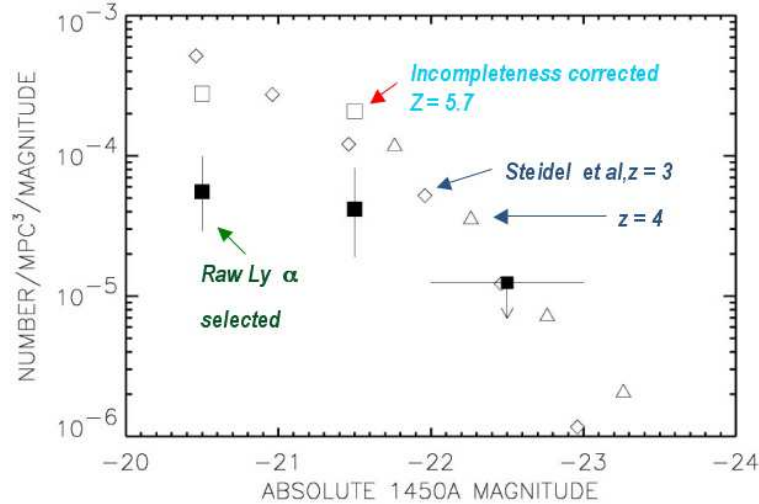


Figure 2. The UV continuum luminosity function of identified $z \sim 5.7$ galaxies (*boxes*) compared with the UV continuum luminosity functions at $z \sim 3$ (*diamonds*) and at $z \sim 4$ reported by Steidel *et al.* (1999). Measured points are shown as *solid boxes* with 1σ Poisson uncertainties based on the number of objects in each bin; the open boxes that match closely to the lower redshift luminosity functions show assumed values if emitters pick out 20% of the LBG sample as Steidel *et al.* (2000) find to be the case at $z \sim 3$.

3. Luminosity Functions

With the high-redshift samples in hand, we can construct luminosity functions at $z \sim 5.7$ and $z \sim 6.5$, and compare these to results at lower redshifts. The most direct comparison is to use the UV continuum luminosities of the Ly α -selected samples and compare these with luminosity functions of the Lyman-break galaxies (Steidel *et al.* (1999), Steidel *et al.* (2000)) at redshifts $z \sim 3$ and $z \sim 4$ (Figure 2). This avoids problems of estimating possible dust contamination on the emission line. Here the main uncertainty is how to correct the raw counts for the fractional population with strong Ly α emission. If the estimate of Steidel *et al.* (2000) based on the LBGs at $z \sim 3 - 4$ with strong Ly α is used to assume that the Ly α emitters represent only 20% of the star-forming galaxy population at $z \sim 5.7$, then the raw numbers for Ly α -selected galaxies (*filled boxes*) are corrected upwards to the *open boxes* that overlie the $z \sim 3$ and $z \sim 4$ Lyman break galaxy UV continuum luminosity functions, implying there has not been a substantial decrease in the star formation rate out to redshift $z \sim 5.7$.

For the $z \sim 6.5$ sample the longest wavelength deep continuum band (z' around 9200 Å) spans the wavelength of Ly α emission, making it difficult to estimate the line-free ultraviolet continuum. Here, we compare the Ly α luminosity function with the luminosity function of the emission line obtained in narrowband samples at $z \sim 3.4$ (Cowie & Hu (1998), Hu *et al.* (1999)). The results are shown in Figure 3. The $z \sim 3.4$ points are plotted with *open boxes* and the $z \sim 5.7$ points are shown with *filled boxes*. The vertical dashed line indicates the limits of the sample, which does not reach the flat part of the $z \sim 5.7$ luminosity function. The *filled box and upper limit drawn with heavy bars* represent the points for the $z \sim 6.5$ luminosity function and overlie the $z \sim 5.7$ luminosity function data. The points are consistent with no marked change in the luminosity function between $z \sim 5.7$

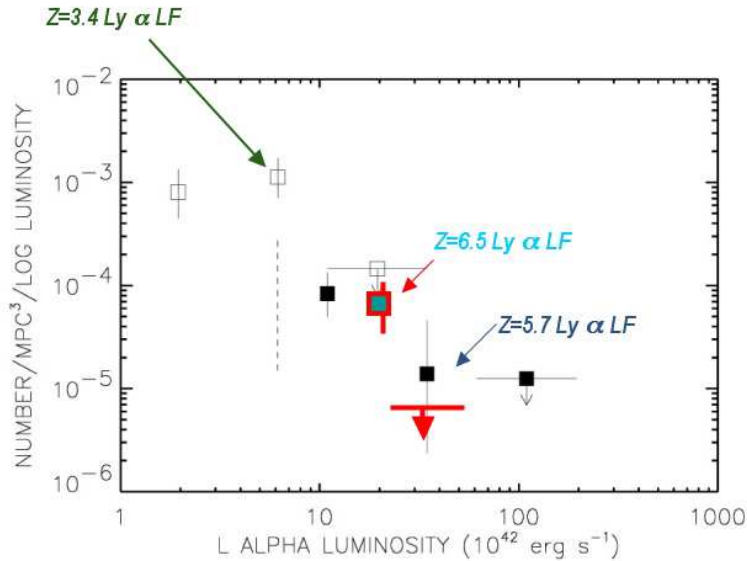


Figure 3. The Ly α luminosity function of identified $z \sim 5.7$ galaxies (*filled boxes*) compared with the Ly α luminosity functions at $z \sim 3.4$ (*open boxes*) (Cowie & Hu (1998), Hu *et al.* (1999)). Measured points are shown with 1σ Poisson uncertainties based on the number of objects in each bin. The vertical dashed line indicates the limits of the $z \sim 5.7$ survey, which does not extend to the faint end of the $z \sim 3.4$ Ly α luminosity function. The points and upper limits for the $z \sim 6.5$ luminosity function are shown with the thick bars, and are consistent with the $z \sim 5.7$ luminosity function, but are based on only 14 galaxies.

and $z \sim 6.5$ as suggested by Malhotra & Rhoads (2004), who used a likelihood analysis to merge disparate data samples with varying degrees of incompleteness to compare the two redshift samples. The advantage of the present results lies in the larger and homogeneous samples, and the completeness of identifications.

4. Ly α Emission Line Profiles

If reionization occurred at redshifts lower than $z = 6.5$ we should see a major change in the equivalent widths of the Lyman alpha emission line between the $z = 6.5$ sample and the $z = 5.7$ sample since the damping wings of the neutral gas should scatter much of the redward wing of the Lyman alpha lines at the higher redshifts where the intergalactic gas is neutral. We can examine the emission-line profiles in the two samples. Figure 4 shows that the Ly α profiles, which have been stacked to improve our sensitivity, are extremely similar. Both profiles show the strong blue asymmetry due to the Ly α forest that is characteristic of the very high-redshift galaxies. The profiles have similar equivalent widths and shapes.

Does this provide clear evidence that the epoch of reionization must lie at higher redshifts? Not necessarily. For Ly α -emitting galaxies that are sufficiently luminous, self-clearing can complicate their effectiveness as a probe of the surrounding neutral IGM (e.g., Haiman (2002)). Even for lower luminosity objects, clustered distributions or neighboring objects may ionize the local region. The $z \sim 6.5$ samples are still relatively small, and show a surprising amount of field-to-field variation, with 10 of the identified systems coming from the A370 field – coincidentally, the first field with a discovered $z > 6$ galaxy (Hu *et al.* (2002)). Preferred (low density) lines of sight could be ionized, and there can

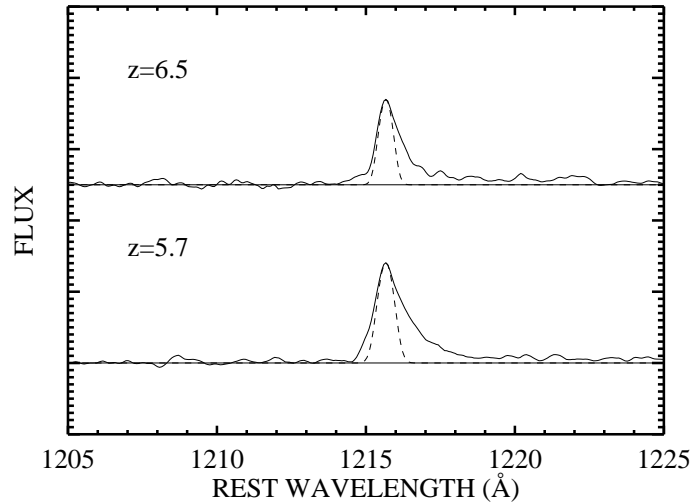


Figure 4. Stacked profiles of identified $z \sim 6.5$ galaxies and $z \sim 5.7$ galaxies. The dotted profile shows the spectral resolution from the night sky lines, and the steep blue fall-off due to absorption by neutral hydrogen is clearly evident in the asymmetric line profile. The profiles are extremely similar in equivalent width (56\AA and 60\AA) and shape. This may suggest that the reionization epoch is at higher redshift, since we might hope to see a change in the profiles due to the expected increase in scattering redward of $\text{Ly}\alpha$ from hydrogen damping wings due to the surrounding neutral medium if we sample galaxies above and below the reionization redshift (suggested at $z \sim 6.2$).

be selection biases in our $z \sim 6.5$ sample. The properties could reflect large-scale structure effects or a porous reionization boundary in both the profile and luminosity function analyses.

5. Large-Scale Structure

The $z \sim 5.7$ spectroscopic samples (Hu *et al.* (2004), Hu *et al.* (2005)) with near-complete coverage in the SSA22 and HDF-N SuprimeCam fields provided the first quantitative demonstration of the existence of structured kinematic and redshift structures on large scales (~ 60 Mpc co-moving distance) at these redshifts. The long diagonal filament in *right panel* of Figure 5 makes up a distinct redshift system with $\text{Ly}\alpha$ emission falling in the bottom quarter of the filter. Such features are also seen in maps of the HDF-N. Similar structured distribution at $z \sim 5.7$ has recently been reported by Ouchi *et al.* (2005) for the Subaru XMM Deep Field.

6. Conclusions

We are now able to obtain large samples of $z \sim 5.7$ and $z \sim 6.5$ galaxies. The continuum and $\text{Ly}\alpha$ luminosity functions seem to be similar to those at lower redshifts, indicating a strong contribution to the ionization of the IGM from star-formation at these redshifts. Both the $\text{Ly}\alpha$ luminosity function and the $\text{Ly}\alpha$ line shapes are similar at $z \sim 5.7$ and $z \sim 6.5$. Large scale structure revealed in the distribution of these high-redshift galaxies leads us to the exciting conclusion that we may be able to make 3-dimensional maps of the cosmic web at these redshifts!

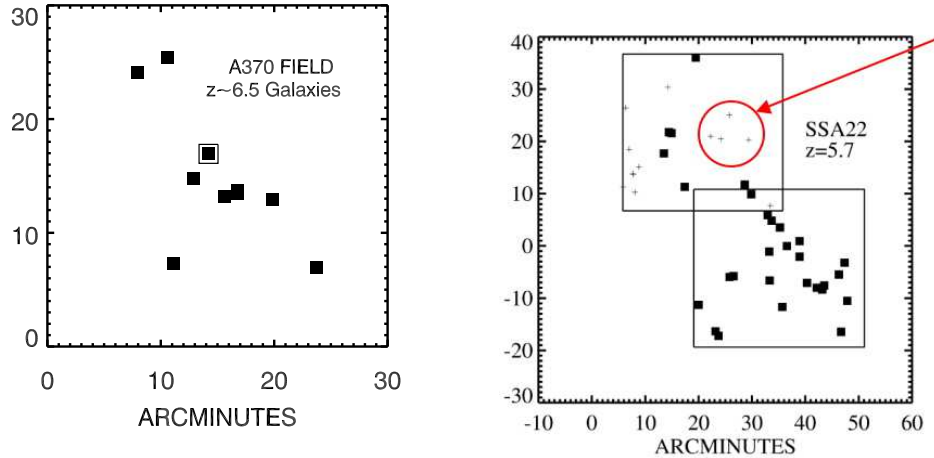


Figure 5. (*Left*) The $z \sim 6.55$ emitters in A370 display a filamentary extent. The box indicates a $z \sim 6.74$ galaxy, currently, the highest confirmed redshift. (*Right*) Redshift $z \sim 5.7$ structure in the expanded SSA22 field. Small crosses (circled region) show candidates not yet spectroscopically observed along the extended filament.

Acknowledgements

This research was supported by NSF grants AST 00-71208 to E.M.H. and AST99-84816 to L.L.C., and by NASA grant GO-7266.01-96A from Space Telescope Science Institute, which is operated by AURA, Inc. under NASA contract NAS 5-26555. We are grateful to the staff of the Keck and Subaru Telescopes for supporting these observations.

References

- Capak, P. *et al.* 2004, *AJ* 127, 180
 Cowie, L.L. & Hu, E.M. 1998, *AJ* 115, 1319
 Haiman, Z. 2002, *ApJ* (Letters) 576, L1
 Hu, E.M., Cowie, L.L., & Capak, P. 2005, *AJ* submitted
 Hu, E.M., Cowie, L.L., Capak, P., Hayashino, T., & Komiyama, Y. 2004, *AJ* 127, 563
 Hu, E.M., Cowie, L.L., & McMahon, R.G. 1999 *ApJ* (Letters) 502, L99
 Hu, E.M., Cowie, L.L., McMahon, R.G., Capak, P., Iwamuro, F., Kneib, J.-P., Maihara, T., & Motoharo, K. 2002, *ApJ* (Letters) 568, L75; Erratum, *ApJ* (Letters) 576, L99
 Kakazu, Y. *et al.* 2005, in preparation
 Malkhotra & Rhoads 2004, *ApJ* (Letters) 617, L5
 Ouchi *et al.* 2005, *ApJ* (Letters) 620, L1
 Spinrad, H. 2004, in: J.W. Mason (ed.), *Astrophysics Update*, (Berlin: Springer-Verlag and Chichester, UK: Praxis Publishing), p. 155, (astro-ph/0308411)
 Steidel, C.C., Adelberger, K.L., Giavalisco, M., Dickinson, M., & Pettini, M. 1999, *ApJ* 519, 1
 Steidel, C.C., Adelberger, K.L., Shapley, A.E., Pettini, M., Dickinson, M., & Giavalisco, M. 2000, *ApJ* 532, 170
 Taniguchi *et al.* 2005, *PASJ* 57, 165